Spectrum Configuration Framework for Throughput Maximization in Open Systems with Roll-Off-Based QoT Optimization

Peyman Pahlevanzadeh[*‡], Venkata Virajit Garbhapu[*], Agastya Raj[*], Dmitrii Briantcev[†], Dan Kilper[†], Marco Ruffini[*]
[*]School of Computer Science and Statistics, ADAPT centre, Trinity College Dublin, Ireland
[†]School of Engineering, CONNECT Centre, Trinity College Dublin, Ireland
[‡]*pahlevap@tcd.ie*

***Abstract*—We propose a spectrum-configuration framework for open and disaggregated optical systems that maximizes throughput while guaranteeing the quality of transmission (QoT) margins. The framework jointly optimizes transceiver parameters, including modulation format, symbol rate, pulse-shaping roll-off factor, and wavelength- selective switch (WSS) bandwidth, under fixed spectral allocation constraints. The impact of roll-off factor optimization is first experimentally evaluated in the presence of cascaded WSS filtering, demonstrating measurable QoT gains for both single- and multi-channel transmission. Building on these observations, a knapsack-based optimization is applied in the context of Optical Spectrum as a Service (OSaaS) to select service configurations that maximize aggregate throughput within a fixed spectrum width and limited transceiver resources. Experimental validation on a metro-scale open testbed confirms the effectiveness of the proposed approach in achieving efficient spectrum utilization and adaptive throughput–margin trade-offs.**

***Index Terms*—Elastic optical networks, optical spectrum as a service, roll-off factor optimization, wavelength-selective switches, and throughput maximization.**

I. Introduction

Optical networks are evolving from fixed-grid architectures toward elastic optical networks (EONs), driven by the increasing demand for data-intensive applications and the need for more efficient spectrum utilization. Unlike fixed 50 or 100 GHz channel spacing, EONs based on flex-grid allow variable-width channels, offering more flexibility. Flexible wavelength-selective switches (flex-WSSs) enable dynamic bandwidth allocation at the channel level [1]. Building on this flexibility and the increased interest in open and disaggregated systems, operators are exploring Optical Spectrum as a Service (OSaaS), in which tenants lease spectrum slices and independently manage their transceivers, with the potential of supporting optical interconnection across heterogeneous domains [2].

A large number of prior work has focused on optimizing the line system, including the configuration of in-line Erbium-Doped Fiber Amplifiers(EDFAs), gain equalization [3], and launch power optimization along the optical link [4]. These approaches primarily target link-level impairments and aim to maximize performance margins by tuning amplifier settings and transmitted power. In contrast, the impact of transceiver-level configuration parameters has received comparatively less attention in open and disaggregated optical systems.

A key challenge in this context is achieving high spectral efficiency without compromising quality of transmission (QoT). The roll-off factor (ROF) of the root-raised-cosine (RRC) pulse-shaping filter remains underexplored despite its critical impact. Increasing the ROF reduces inter-symbol interference (ISI) but also expands the occupied bandwidth [5], [6]. In addition, the ROF directly affects tolerance to residual impairments such as skew [7]. This trade-off is particularly critical for higher-order modulation formats, such as DP-64QAM, where increased ISI sensitivity can severely degrade QoT. Selecting appropriate ROF and WSS bandwidth can therefore mitigate filtering penalties and improve performance margins without requiring additional hardware. Proprietary systems typically rely on vendor-specific planning and engineering tools to determine optimized system and transceiver configurations. In contrast, open tools for disaggregated systems, such as GNPy [8], primarily focus on transmission performance and generally lack mechanisms for optimizing transceiver parameters such as modulation format, symbol rate, and pulse-shaping roll-off factor. In this work, we first experimentally evaluate the impact of ROF on QoT for different modulation formats and symbol rates under WSS filtering constraints. We then introduce a spectrum-configuration framework for OSaaS that jointly optimizes transceiver parameters to configure a fixed spectral allocation with guaranteed QoT margins while maximizing overall throughput. The proposed approach provides a practical, measurement-driven solution for efficient and high-throughput operation in OSaaS-based EONs.

II. Methodology

In OSaaS or open line systems (OLS), a tenant acquires a fixed spectral band (e.g., $W = 300$ GHz) and either the tenant (OSaaS) or operator (OLS) must configure it to maximize throughput while guaranteeing QoT. The tenant has: (i) a service catalog of modulation formats m_S and symbol rates R_s, (ii) N_{TRx} transceivers, (iii) topology information (number of Reconfigurable Optical Add/Drop Multiplexers(ROADMs)

978-3-903176-78-2 © 2026 IFIP

and EDFAs, and, where possible, (iv) a Generalized Signal-to-Noise Ratio (GSNR) spectral profile from QPSK probing. All selected channels must meet $Q_{\text{target}}(m) = Q_{\text{FEC}}(m) + \Delta Q_{\text{margin}}$ [9]. Our framework comprises five stages (Fig. 1).

Stage 1: GSNR Profiling. We sweep a QPSK probe signal across the allocated spectrum [10], measure the frequency-dependent BER, and convert it to a GSNR profile, $\text{GSNR}(f)$. Given the target margin ΔQ_{margin}, this GSNR profile is used to determine the set of feasible services that can be supported at each spectral location. Specifically, for each modulation format and symbol rate in the service catalog, we verify whether the corresponding QoT requirement Q_{target} can be satisfied. This process identifies, across the spectrum under test, which combinations of modulation format and symbol rate are eligible for deployment under the desired QoT margin.

Stage 2: Service Configuration. For each feasible service (m_s, R_s), we determine two components: (i) optimal ROF $\alpha^*(m)$ from pre-characterized transceiver data (vendor-provided or experimentally obtained), and (ii) *minimum WSS bandwidth* b^* via simulation using the WSS model [11]. The simulator estimates the occupied bandwidth $B_{\text{occ}}(R_s, \alpha^*)$ through time-domain signal generation and power spectral density computation, then uses a cascade model $B_{\text{eff}}^{(3\text{dB})}(N_{\text{WSS}}, b)$ to select the smallest b^* satisfying $B_{3\text{dB}}(N_{\text{WSS}}, b^*) \geq B_{\text{occ}}(R_s, \alpha^*)$. This ensures the signal fits within the effective passband after N_{WSS} cascaded filters without clipping. Each service is recorded as $(m_s, R_s, \alpha^*, b^*)$ with throughput $v_s = 2R_s \log_2(M(m_s))$ and bin cost $k_s = \lceil b^*/g \rceil$, where $g = 6.25$ GHz is the WSS granularity. The throughput v_s represents the gross symbol rate; the net client data rate accounts for 27% SD-FEC overhead. Since the SD-FEC overhead is fixed at 27% across all services, we omit this factor from the optimization formulation without loss of generality.

Stage 3: Knapsack Packing. The available spectrum is discretized into $B = \lceil W/g \rceil$ frequency bins, and the service selection problem is formulated as a two-dimensional bounded knapsack optimization. The objective is to maximize the aggregate throughput $\sum x_s v_s$ subject to a spectrum constraint $\sum x_s k_s \leq B$ and a transceiver constraint $\sum x_s \leq N_{\text{TRx}}$. The problem is solved using dynamic programming, with the state $\text{DP}[b][t]$ representing the maximum achievable throughput using b spectrum bins and t transceivers.

Fig. 2 illustrates the output of the knapsack optimization, showing the maximum achievable throughput versus the number of transceivers for different GSNR profiles within a fixed 200 GHz spectral window. The circles indicate the service configurations selected by the optimizer, including the modulation format and symbol rate determined in Stage 2. An important observation is that increasing the number of transceivers does not necessarily lead to higher throughput. For example, for a GSNR profile of 18 dB, deploying three transceivers yields a higher total throughput than using four transceivers, as the additional channel must operate at a more conservative service configuration to satisfy the QoT constraint. This highlights the benefit of jointly optimizing

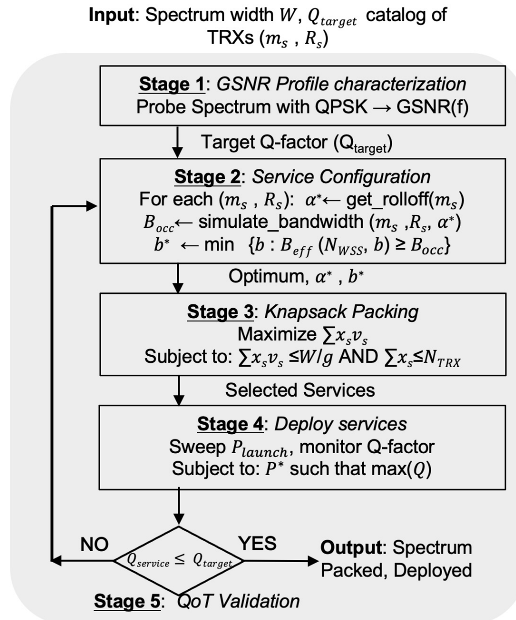

Fig. 1. Workflow of the proposed spectrum-configuration framework for OSaaS and open line systems, comprising GSNR profiling, service configuration, knapsack-based spectrum packing, deployment with launch-power optimization, and QoT monitoring.

spectrum allocation and transceiver parameters, rather than maximizing the number of deployed channels.

Stage 4: Deployment & Power. After deploying the selected channels, we sweep the transmitter booster gain and measure the Q-factor of all channels. In OSaaS systems, users have no control over in-line EDFAs along the lightpath; thus, launch power optimization is limited to the booster EDFA at the transmitter side.

Stage 5: Monitoring. After deploying the selected channels, we monitor the Q-factor of all channels. If $Q_{\text{measured}} < Q_{\text{target}}$, the spectrum allocation is deemed infeasible, and Stage 2 is re-run to select the next-best feasible service configuration. This iterative process continues until the QoT requirement is satisfied.

Optimization Problem Formulation

Let $\mathcal{S}$ denote the set of feasible services obtained from Stage 2. Each service $s \in \mathcal{S}$ is characterized by a throughput $v_s = 2R_s \log_2(M_s)$ and a required WSS bandwidth b_s. The corresponding spectrum cost in discrete bins is $k_s = \lceil b_s/g \rceil$, where g denotes the WSS granularity. The total available spectrum is W, yielding $B = \lceil W/g \rceil$ spectrum bins, and N_{TRx} transceivers are available.

We define the binary decision variable

$$x_s = \begin{cases} 1, & \text{if service } s \text{ is selected,} \\ 0, & \text{otherwise.} \end{cases} \tag{1}$$

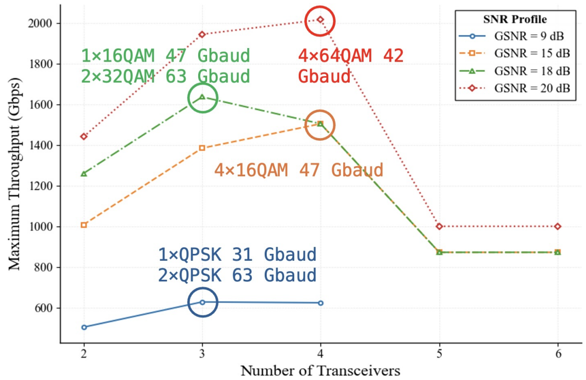

Fig. 2. Maximum throughput versus number of transceivers for different GSNR profiles of the link in the fixed 200 GHz spectrum. Circles indicate the service configurations (modulation format and symbol rate) selected by the knapsack optimization.

The optimization problem is formulated as

$$\max_{\{x_s\}} \quad \sum_{s\in\mathcal{S}} v_s x_s \tag{2}$$

$$\text{s.t.} \quad \sum_{s\in\mathcal{S}} k_s x_s \leq B, \tag{3}$$

$$\sum_{s\in\mathcal{S}} x_s \leq N_{\text{TRx}}, \tag{4}$$

$$x_s \in \{0,1\}, \quad \forall s \in \mathcal{S}. \tag{5}$$

Only services satisfying the QoT requirement $Q_{\text{measured}} \geq Q_{\text{target}}$ are included in $\mathcal{S}$. Consequently, QoT constraints are enforced implicitly by construction.

III. Experimental Setup

To characterize the impact of ROF optimization in the presence of WSS filtering, we first consider a single-channel experimental setup. The testbed comprises a commercial Adtran Teraflex coherent transceiver employing RRC pulse shaping at the transmitter, followed by a MUX-side WSS, a booster EDFA, 70 km of standard single-mode fiber, a pre-amplifier EDFA, a DEMUX-side WSS, and a receiver with standard DSP. This configuration allows controlled evaluation of how the transmitted signal, constrained by a finite WSS passband, is affected by changes in ROF The experimental characterization of single-channel ROF optimization and its impact on QoT is presented and discussed in Section IV.

In the second step as shown in Fig. 4(b), we extend the analysis to a multi-channel scenario to evaluate the effectiveness of ROF optimization in an OSaaS context. We deploy four Teraflex transceivers within a fixed 300 GHz spectral window and consider a metro-style topology comprising a MUX and DEMUX at the transmitter and receiver, respectively, and one intermediate ROADM to introduce additional filtering effects. The total link length is approximately 175 km. In this scenario, we jointly optimize the ROF and the launch power of the transmitter-side booster EDFA for all four channels. Finally, to evaluate the framework under more severe filtering conditions as shown in Fig. 4(a), we consider a third scenario with two ROADMs along the lightpath, resulting in a total of six cascaded WSSs. This configuration further accentuates bandwidth-narrowing effects and is used to validate the proposed workflow under strong filtering constraints. The experimental results for this scenario are also presented and discussed in Section IV.

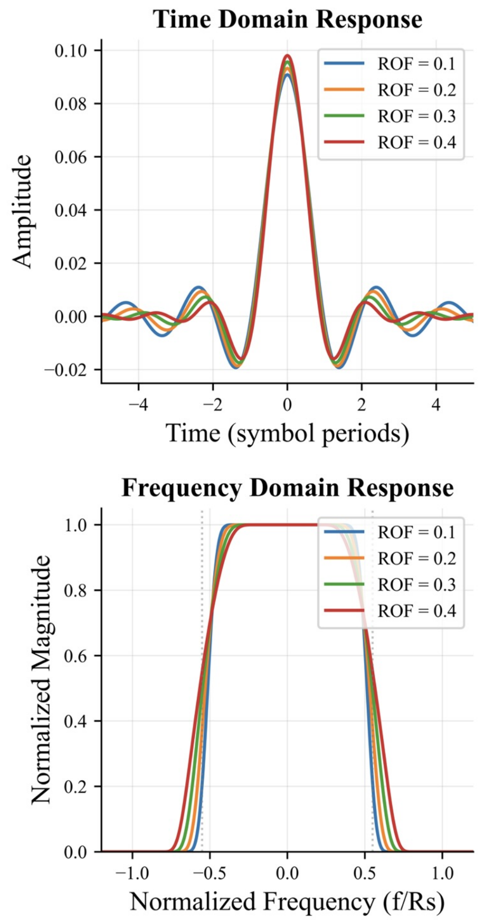

Fig. 3. RRC pulse shaping in the time and frequency domains for different roll-off factors.

IV. Results and Discussion

Fig. 3 illustrates the effect of the ROF on RRC pulse shaping in the time and frequency domains. The top plots show the impulse responses of the RRC filter for different ROF values. As the ROF increases from 0.1 to 0.4, the temporal sidelobes of the pulse decay more rapidly, indicating reduced ISI. The bottom plots of Fig. 3 present the corresponding frequency responses of the RRC filter. Increasing the ROF leads to a wider occupied bandwidth, reflecting the trade-off between time-domain compactness and spectral efficiency. In the presence of cascaded WSS filtering, this bandwidth expansion can increase susceptibility to filtering penalties. Therefore, understanding the joint impact of ROF on both time-domain compactness and spectral occupation is

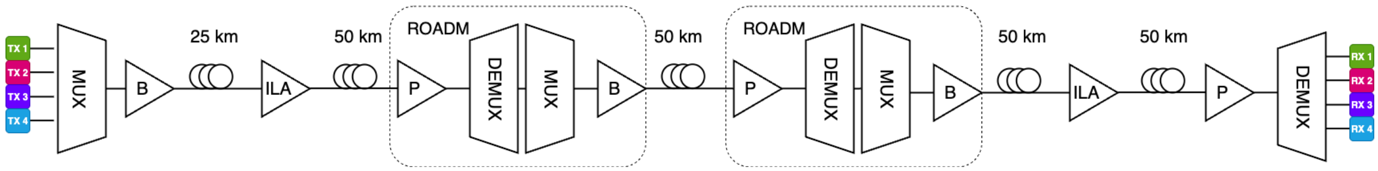

(a) Topology A

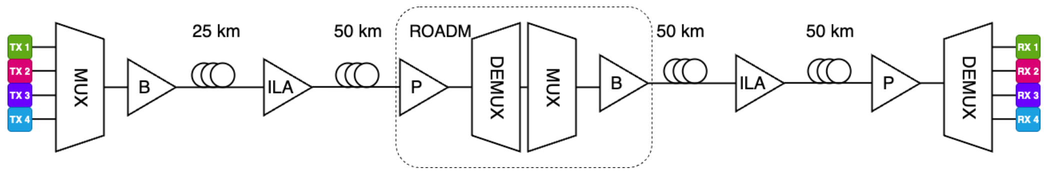

(b) Topology B

Fig. 4. Topologies used to evaluate ROF optimization and spectrum-configuration performance. (a) Five-span configuration with 6 WSSs. (b) Four-span configuration with 4 WSSs.

TABLE I

EXPERIMENTAL RESULTS OF THE SPECTRUM UNDER TEST(SUT) CONFIGURATIONS.

Knapsack Opt.	SUT (GHz)	#TRXs	GSNR (dB)	Mod.	Sym. Rate (Gbaud)	ROF	WSS BW (GHz)	Q-Fact (dB)	Cap. (Gbps)
4×64QAM–42G	200	4	19.91	**64QAM**	**42**	0.35	50	6.87	**2016**
	200	4	19.88	64QAM	31	0.35	50	6.87	1488
	200	4	18.97	32QAM	37	0.30	50	9.05	1480
4×32QAM–63G	300	4	17.85	**32QAM**	**63**	0.20	75	7.90	**2520**
	300	4	19.53	64QAM	52	0.40	75	6.40	2496
	300	4	16.08	16QAM	63	0.15	75	9.17	2016

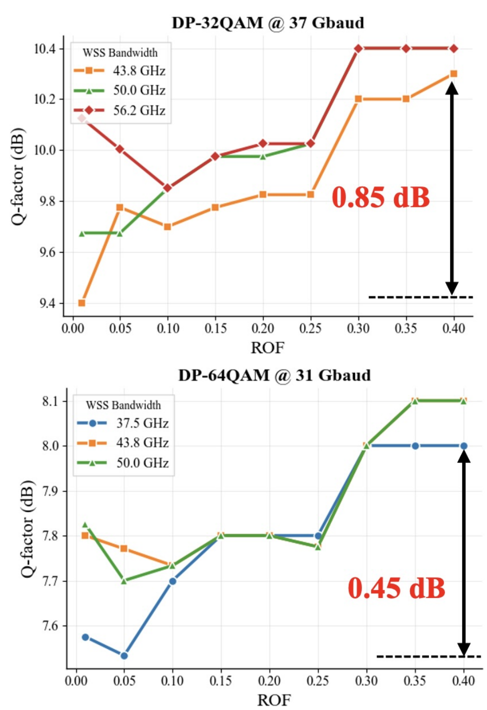

Fig. 5. Measured Q vs. ROF for single channel DP-64QAM@31 GBd and DP-32QAM@37 GBd across WSS bandwidths

essential for evaluating system performance under realistic WSS-constrained transmission conditions. Fig. 5 presents the measured Q-factor as a function of the ROF for different WSS bandwidths, obtained from the single-channel experiments conducted using the setup described in Section III. The results are shown for DP-32QAM at 37 GBd (top) and DP-64QAM at 31 GBd (bottom). Increasing the ROF leads to improved Q-factor for both modulation formats. In particular, for DP-32QAM, ROF optimization yields up to 0.85 dB improvement in Q-factor under narrow WSS filtering, while for DP-64QAM a maximum gain of approximately 0.45 dB is observed.

The contour plots shown in Fig. 6(a) present the average Q-factor of four channels tested in the topology of Fig. 4(b) with four cascaded WSSs. We assumed a 300 GHz spectral budget and loaded four channels. In *Scenario 1*, each channel carried DP-16QAM at 63 Gbaud, mapped to a 75 GHz WSS window with zero guard band. In *Scenario 2*, each channel carried DP-32QAM at 50 Gbaud, again using a 75 GHz WSS window across all MUX/DEMUX elements along the lightpath. The optimization jointly tuned the ROF and the transmitter booster launch power. The contour plots illustrate the joint dependence of Q-factor on relative launch power and ROF, where relative launch power denotes the difference between the actual launch power and the optimum launch power. Fig. 6(a) shows the measured Q-factor trends for DP-16QAM due to its lower-order modulation, ISI sensitivity is reduced, and the best operating point occurs at a moderate roll-off of ROF $\approx [0.15, 0.2]$. For DP-32QAM shown in Fig. 6(b), ISI is more pronounced, and increasing the ROF improves QoT;

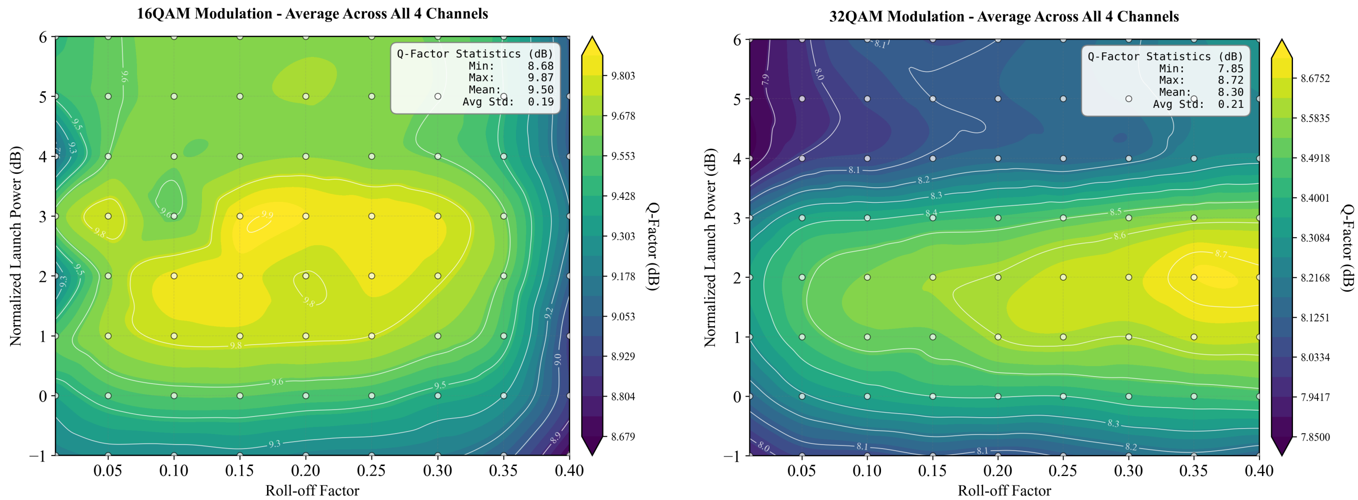

(a) DP-16QAM optimum configuration

(b) DP-32QAM optimum configuration

Fig. 6. Optimum roll-off and launch-power operating points under WSS filtering for (a) DP-16QAM and (b) DP-32QAM.

the optimum occurs at $\mathrm{ROF} \approx [0.35, 0.4]$. In both scenarios, the Q-factor improves with increasing launch power until NLI becomes dominant, beyond which further increases degrade QoT. Table I presents the experimental results obtained from the 6-WSS topology shown in Fig. 4(a). The first row for each SUT represents the optimal configuration predicted by the knapsack optimizer. Additional modulation format and symbol rate combinations were tested around these configurations to verify that the solutions were indeed optimal. As observed, the configurations achieving the highest throughput align with the optimizer's predictions. For the 200 GHz allocation, the optimizer correctly identifies DP-64QAM at 42 Gbaud as the maximum-capacity solution (2016 Gbps). However, with a measured Q-factor of 6.87 dB, this configuration operates near the FEC threshold. Suppose the user's margin requirement is not satisfied. In that case, the framework iteratively selects the next-best solution: DP-32QAM at 37 Gbaud, which provides a Q-factor of 9.05 dB with a sufficient margin at a throughput of 1480 Gbps, demonstrating the adaptive throughput-margin trade-off.

V. Conclusions

We presented a spectrum-configuration framework for OSaaS and open line systems that maximizes throughput by jointly optimizing transceiver parameters, including modulation format, symbol rate, and pulse-shaping roll-off factor. Experimental validation on the OpenIreland testbed demonstrates that proper ROF tuning yields measurable Q-factor improvements under cascaded WSS filtering, with gains up to 0.85 dB. The knapsack-based optimization effectively balances throughput and margin requirements, enabling adaptive service selection within fixed spectral allocations. The proposed framework provides a practical, measurement-driven approach for tenants and operators to maximize spectral efficiency in optical networks without additional hardware investment.

Acknowledgments. Work supported by research grants from Research Ireland under 22/FFP-A/10598, 18/RI/5721, 13/RC/2077 P2, 13/RC/2106 P2.

References

[1] J. M. Fabrega, M. S. Moreolo, L. Martín, A. C. Piat, E. Riccardi, D. Roccato, N. Sambo, F. Cugini, L. Potì, S. Yan, E. Hugues-Salas, D. Simeonidou, M. Gunkel, R. Palmer, S. Fedderwitz, D. Rafique, T. Rahman, H. de Waardt, and A. Napoli, "On the filter narrowing issues in elastic optical networks," *Journal of Optical Communications and Networking*, vol. 8, no. 7, pp. A23–A33, 2016.

[2] K. Kaeval, K. Grobe, and J.-P. Elbers, "Operation of optical spectrum as a service in disaggregated and multi-operator environments [invited]," *Journal of Optical Communications and Networking*, vol. 17, no. 1, pp. A46–A58, 2025.

[3] G. Borraccini, A. D'Amico, S. Straullu, F. Usmani, A. Ahmad, and V. Curri, "Iterative supervised learning approach using transceiver bit-error-rate measurements for optical line system optimization," *Journal of Optical Communications and Networking*, vol. 15, no. 2, pp. 111–118, 2023.

[4] A. Mitra, D. Semrau, N. Gahlawat, A. Srivastava, P. Bayvel, and A. Lord, "Effect of channel launch power on fill margin in c+l band elastic optical networks," *Journal of Lightwave Technology*, vol. 38, no. 5, pp. 1032–1040, 2020.

[5] K. Harako, D. Suzuki, T. Hirooka, and M. Nakazawa, "Roll-off factor dependence of nyquist pulse transmission," *Opt. Express*, vol. 24, no. 19, pp. 21 986–21 994, Sep 2016. [Online]. Available: https://opg.optica.org/oe/abstract.cfm?URI=oe-24-19-21986

[6] P. Pahlevanzadeh, "Innovative solutions for coherent transmission in optical access networks," Master's thesis, Politecnico di Torino, 2024. [Online]. Available: https://webthesis.biblio.polito.it/34100/

[7] Y. Yue, Q. Wang, and J. Anderson, "Transmitter skew tolerance and spectral efficiency tradeoff in high baud-rate qam optical communication systems," *Opt. Express*, vol. 26, no. 12, pp. 15 045–15 058, Jun 2018. [Online]. Available: https://opg.optica.org/oe/abstract.cfm?URI=oe-26-12-15045

[8] V. Curri, "Gnpy model of the physical layer for open and disaggregated optical networking [invited]," *Journal of Optical Communications and Networking*, vol. 14, no. 6, pp. C92–C104, 2022.

[9] Y. Pointurier, "Design of low-margin optical networks," *Journal of Optical Communications and Networking*, vol. 9, no. 1, pp. A9–A17, 2017.

[10] K. Kaeval *et al.*, "Employing channel probing to derive end-of-life service margins for optical spectrum services," *JOCN*, 2023.

[11] C. Pulikkaseril *et al.*, "Spectral modeling of channel band shapes in wavelength selective switches," *Opt. Express*, 2011.